JOURNAL OF MATERIALS SCIENCE 32 (1997) 6533–6538

# Measurement of the mechanical properties of a fibre-reinforced composite on the submicrometre scale

F. S. SHIEU
*Institute of Materials Engineering, National Chung Hsing University, Taichung 402, Taiwan*
W. M. LEE
*Department of Chemistry, Western Kentucky University, Bowling Green, KY 421201, USA*

Ultramicrotomy is being used routinely as a sample preparation technique for transmission electron microscopy (TEM). TEM study of thin sections of a diketone-bis-benzocyclobutene composite reinforced with Celion (trademark of BASF Co.) carbon fibre revealed two types of periodic crack in the fibre. Coarse cracks were due to bending at knife tip in the early stage of the ultramicrotomy. Also, very fine cracks were observed near the fibre–matrix interface and believed to have been induced by the shear lags between the fibre and the matrix. A simple analysis indicated that the coarse and fine crack spacings could be used to obtain the compressive strength of the fibre and the ultimate shear stress at the fibre–matrix interface, respectively. The combination of ultramicrotomy and TEM provides a useful tool to explore the mechanical properties of a composite material on the submicrometre scale, in addition to the other microstructural and compositional information accessible by TEM.

## 1. Introduction

The advance of modern technologies relies heavily on the development of new materials having superior properties, such as high strength and toughness. Progress comes from our understanding of the microstructure and chemistry of materials, together with their relationship to properties. This enables an engineer to design a material which meets specific application needs. Transmission electron microscopy (TEM), first invented in 1930s, has made significant contributions to the field of materials science and related fields. Today TEM provides not only the microstructure and crystallinity but also the chemical composition and electronic structure of materials.

To enhance the versatility of conventional monolithic materials, composite materials exhibiting synergetic properties have become a new class of engineering materials. Interfaces play a key role in controlling the performance of a composite material. There has been much research done on the interfaces of composite materials, as reflected in the number of conference proceedings on this topic, e.g., [1–4]. Efforts are made to tailor the interface structure and chemistry to improve material properties. For example, the ductility of $Ni_3Al$ is improved by adding a small amount of boron, as a result of the segregation of a fraction of a monolayer of boron to the grain boundary of $Ni_3Al$ [5]. The shear strength of the NiO–Pt interface is increased by a factor of 4 with the formation of an intermetallic compound NiPt at NiO–Pt interfaces [6]. Structure–property relationships established on the submicrometre scale are, therefore, crucial for the success of tomorrow's technology today.

In this paper, a quantitative method of measuring the compressive strength of a Celion (trademark of BASF Co.) carbon fibre and the ultimate shear stress at the carbon fibre–diketone-bis-benzocylobutene (DK-BCB) interface is reported. This technique requires ultramicrotomy for sample preparation and TEM for imaging the fine structures on the submicrometre scale. A diamond knife in an ultramicrotome functions as the probe for creating cracks in the fibre. Two different cracks (coarse and fine) were observed by TEM, resulting from the different interaction mechanisms between the diamond knife and the composite. Analysis of the details involved in the ultramicrotomy suggests that the compressive strength of the fibre and the ultimate shear stress of the fibre–matrix interface can be obtained from the coarse and fine crack spacings, respectively.

## 2. Analysis of the interactions between the diamond knife and the composite

Sample preparation of a polymer-containing material for TEM observation is usually carried out by ultramicrotomy, in which a block of specimen to be sectioned is trimmed or ground into the shape of a trapezoid. The trapezoid is then cut in an ultramicrotome, using a sharp diamond knife, into a thin section about 100 nm thick. A schematic diagram of

0022–2461  

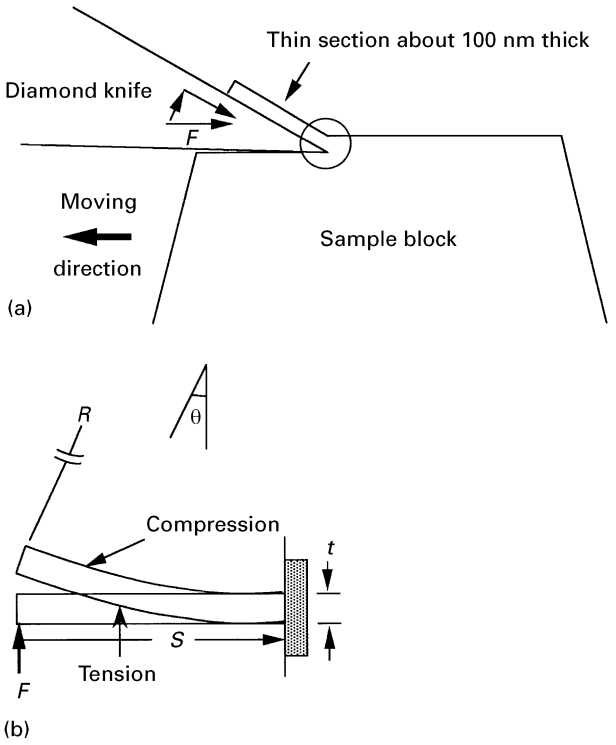


*Figure 1* (a) A schematic diagram of the side view of an ultramicrotome with diamond knife and sample block. (b) The bending of a thin section at the knife tip is simulated by a curved cantilever beam where the upper and lower surfaces are under compression and tension, respectively.

the trapezoid and the diamond knife in an ultramicrotome is shown in Fig. 1a. An applied force $F$ moves the trapezoid against the knife edge and sections the specimen into thin slices. As a result of the knife geometry, bending of thin sections occurred at the knife tip when the specimen begins to contact with the diamond knife. This is, for a first approximation, similar to a curved cantilever beam (or plate) with a radius, $R$, of curvature and subtended angle, $\theta$, shown in Fig. 1b, where the upper surface of the beam is under compression, while the lower surface is under tension.

For an elastic material, the maximum strain at outer surfaces can be calculated from the thickness $t$, of the beam (or plate), and the radius $R$, of curvature by the relation

$$\varepsilon = \frac{t}{2R} \tag{1}$$

The maximum stress is related to the maximum strain by Hooke's law, i.e.,

$$\sigma = E\varepsilon \tag{2}$$

where $E$ is Young's modulus of the material. The length, $S$, of the cantilever beam is related to the radius $R$, of curvature, and subtended angle, $\theta$, by

$$S = R\theta \tag{3}$$

Solving Equations 1–3 gives rise to

$$s = \frac{Et\theta}{2S} \tag{4}$$

During ultramicrotomy the lower surface of the thin section contacting the diamond knife is supposed to be under tension, corresponding to the convex side of the curved cantilever beam in Fig. 1b. In practice, this tension is slightly offset by the shear stress resulting from the parallel component of the applied force (see Fig. 1a). Therefore, the compressive stress at upper surface of the thin section should be higher than the tensile stress at the lower surface. Consequently a brittle material under this condition would fail by the compression rather than by the tension mode. Fracture of the material occurs when the maximum compressive stress at upper surface reaches the compressive strength, $\sigma_f$, of the material. Once a crack is developed, the compressive stress is temporarily released and the thin section moves forwards. The whole process will be repeated regularly, resulting in a periodic crack in the brittle material. Each broken segment between cracks resembles a curved cantilever beam while it was seated at the knife tip. Hence the compressive strength, $\sigma_f$, of the material can be obtained from the measured cracking space, $\lambda$, using Equation 4 with $\sigma_f$ and $\lambda$ substituted for $\sigma$ and $S$, respectively, i.e.,

$$\sigma_f = \frac{Et\theta}{2\lambda} \tag{5}$$

As discussed, bending at the knife tip is the mechanism for the failure of brittle materials; there is another possible mechanism which can generate stresses and cause fracture in the brittle component of a composite during ultramicrotomy. When a thin section of the composite passes the knife tip, it immediately experiences a shear stress at the lower surface, i.e., the thin section–knife interface, resulting from the parallel component of the applied force, $F$, as indicated in Fig. 1a. This applied shear stress will induce another shear stress in the vicinity of the fibre–matrix interface due to a shear lag between the fibre and the matrix. This induced shear stress is caused by the difference between the shear moduli of the fibre and the matrix, as illustrated in Fig. 2.

The top view of a thin section composed of one fibre, parallel to the sectioning direction, in a polymer matrix, during ultramicrotomy, is given in Fig. 3. The induced shear stress at the fibre–matrix interface has a maximum near the edge of the fibre where the difference between the displacements of the fibre and the matrix is maximum. A load (compressive stress) is transferred via the induced shear stress from the matrix to the fibre. As the compressive stress accumulates and reaches the fracture strength, $\sigma_{ff}$, of the fibre a crack will be developed in the fibre. It is assumed that the induced shear stress is uniform across the thickness of the thin section and so is the compressive stress throughout the transverse direction of the fibre. If the normal tensile stress at the fibre–matrix interface near the edge does not cause delamination, the compressive stress in the fibre is coupled to the shear stress at the interface through the integral equation

$$\sigma(x)wt = 2t \int_0^x \tau(x)\,\mathrm{d}x \tag{6}$$

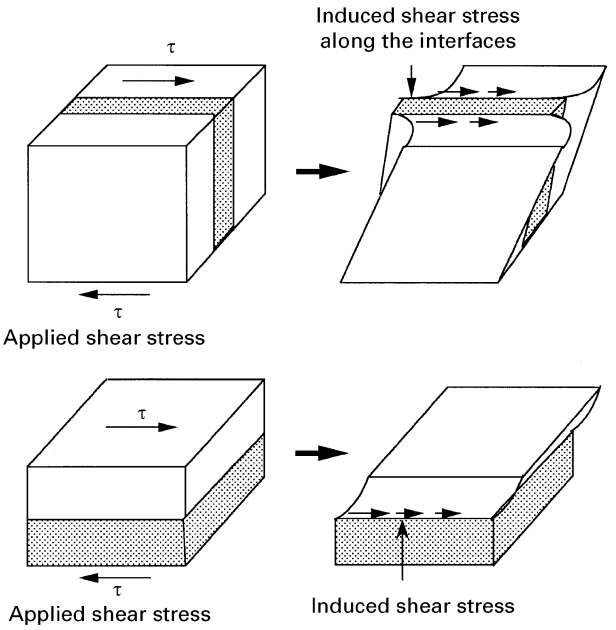


*Figure 2* The response of a laminated composite to an applied shear force. Two types of deformation geometry are possible. In the upper case, the fibre–matrix interfaces are perpendicular to the applied force while, in the lower case, the interface is parallel to the applied force. As a result of the difference between the shear moduli of the two constituents, an induced shear stress is developed at the interfaces.

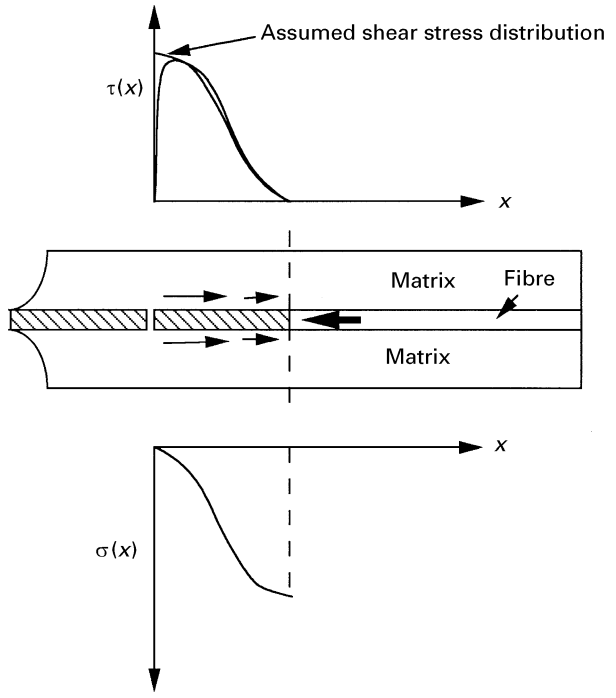


*Figure 3* A top view of the thin section in the ultramicrotome in Fig. 1, illustrating the coupling of the compressive stress in the fibre to the induced shear stress at the fibre–matrix interfaces. The fibre on the sectioned portion (left) is assumed to have interfaces perpendicular to the section surface.

where $\sigma(x)$ is the compressive stress in the fibre, $w$ is the sectioned fibre chord length, $t$ is the thickness of the thin section, $\tau(x)$ is the induced shear stress at the fibre–matrix interface and $x$ is the coordinate along the interface with its origin at the edge. The left-hand side of the equation represents the compressive force in the fibre, i.e., the compressive stress multiplied by the cross-section of the fibre, which should be balanced by the shear force, i.e., the induced shear stress multiplied by the interface area, exerted on the fibre–matrix interface, as given on the right-hand side of the equation.

Although the shear stress distribution at the fibre–matrix interface under the applied compressive force, $F$, is not known and has not been studied, there is a great similarity between the present case and that of a brittle thin film on a ductile substrate under an applied tensile force, which has been explored [6–11]. For the latter, different forms of the shear stress distribution have been proposed. Cox [7] and Dow [8] used a proportional shear lag analysis. Kelly [9] discussed a situation where the matrix can undergo plastic flow, and the shear stress at the interface is considered to be uniform. Agrawal and Raj [10] used a sinusoidal shear stress distribution where the maximum shear stress was located at one quarter of a segment length away from the edge of the crack. Shieu *et al.* [6] used a sinusoidal shear stress distribution with the maximum shear stress located near the edge of the segment in their analysis, based on the experimental results of Tyson and Davis [11].

It is believed that a more realistic shear stress distribution is likely to be that with a maximum shear stress not far from the edge, as shown in Fig. 3. A sinusoidal wave with singularity at the edge was assumed for the present analysis, similar to that of Shieu *et al.* [6]. If failure of the fibre is due to this mechanism, i.e. the accumulated compressive stress in the fibre reaches the fracture strength, $\sigma_{ff}$, of the fibre, the fibre will crack. Again this process will be repeated until the thin section leaves the diamond knife and a periodic crack is present in the fibre. Thus the maximum shear stress, $\tau_{max}$, is obtained by solving Equation 6:

$$\tau_{max} = \frac{\pi w \sigma_{ff}}{4\lambda} \tag{7}$$

where $\lambda$ is the measured crack spacing, which is different from that in Equation 5 for the coarse cracks. It must be borne in mind that the calculated maximum shear stress at the fibre–matrix interface will depend upon the shape of the shear stress distribution, resulting in a different constant in the above equation.

## 3. Experimental procedure and discussion

### 3.1. Determination of the radius, *R*, of curvature, and the subtended angle, θ

In order to measure the compressive strength from the crack spacing using Equation 5, one needs to know the subtended angle, θ, or the radius, $R$, of curvature. Amorphous silica ($SiO_2$) with a known compressive strain of 0.28% [12] was used to obtain these parameters. A multilayer specimen composed of perfluorocyclobutene (PFCB) and aluminium layers on an oxidized Si wafer was prepared by ultramicrotomy for TEM examination. A cross-section transmission

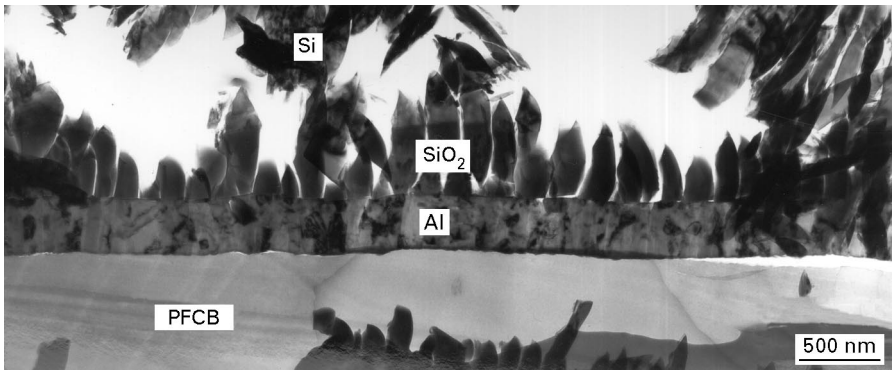


*Figure 4* A cross-section view of the PFCB/Al/$SiO_2$/Si multilayer structures. Fracture of the $SiO_2$ is due to the bending of the brittle amorphous silica at the knife tip.

electron micrograph of the layer structures is shown in Fig. 4. Fragmentation of the amorphous silica occurred during ultramicrotomy and a periodic crack in the $SiO_2$ was observed in the transmission electron micrograph in Fig. 4. The average crack spacing (segment length) is measured to be $322 \pm 41$ nm, which gives a subtended angle, $\theta$, of 18 mrad and a radius, $R$, of curvature of 17.9 mm.

In principle, the cutting speed could change the radius of curvature at the knife tip. However, experiments using different cutting speeds of 10 and 30 mm $s^{-1}$ showed no significant change in the crack spacing of the amorphous silica.

### 3.2. Measurement of the compressive strength of the Celion carbon fibre

Application of this technique to measure the compressive strength of a carbon fibre and the maximum shear stress at the fibre–matrix interface is demonstrated below and in the next section. A composite made of Celion carbon fibre in a DK-BCB matrix was used in this study and prepared for TEM by ultramicrotomy in the same conditions as those for the amorphous silica, with the fibre axis approximately parallel to the sectioning direction. An electron micrograph showing the microstructure of the carbon–(DK-BCB) composite is given in Fig. 5a. It can be seen that all the fibres have broken into regular short segments, as a result of the bending at the knife tip during ultramicrotomy. The average segment length was measured to be $434 \pm 117$ nm. Since the geometry of the diamond knife and the trapezoid is fixed, the subtended angle, $\theta$, is assumed to be 18 mrad, the same as in the amorphous silica. On the basis of this value, the radius of curvature at the knife tip for the fibre is calculated to be 24 mm from Equation 3. If the thickness of the thin section is 100 nm, the fracture strain of the Celion carbon fibre is calculated to be 0.21% from Equation 1. By multiplying the strain by Young's modulus of the fibre, 234 GPa, the compressive strength of the fibre is found to be 491 MPa, which is about an order of magnitude smaller than the tensile strength, 3.79 GPa, provided by the supplier.

It is also noted that the crack spacing of the fibre in the centre of the micrograph (Fig. 5a) is larger than that of fibre at the top. Since the two edges of the fibre in the centre of the micrograph are parallel across its length, this suggests that the fibre was sectioned along the fibre axis. In contrast, the fibre at the top of the micrograph with two sloping edges was cut with the fibre axis inclined to the sectioning direction. The difference in the crack spacings reflects the anisotropy in the mechanical properties of the fibre, i.e., Young's modulus and fracture strength.

### 3.3. Measurement of the maximum shear stress at the fibre–matrix interface

A close look of the fibre at the top of the micrograph in Fig. 5a indicates the presence of fine cracks along both sides of the fibre. These fine cracks are also present in the fibre at the bottom of the micrograph. An enlargement of the fine cracks in the upper fibre of Fig. 5a is shown in Fig. 5b. Since the thickness of the TEM thin section is about 100 nm, far smaller than the fibre diameter, 7 μm as measured by scanning electron microscopy (SEM) before ultramicrotomy, the TEM micrograph in Fig. 5a contains fibres with different chord lengths.

It is evident that the fibre having a chord length of 6.0 μm in the middle of Fig. 5a was cut close to the centre of the fibre; so that the fibre–matrix interfaces are approximately perpendicular to the surface and a distinct and straight boundary between the fibre and the matrix is expected (Fig. 6a). Whereas the sectioned fibre at the top of Fig. 5a has chord lengths of 3 μm, the fibre–matrix interfaces are curved (Fig. 6b). In this instance, the average height of the truncated fibre segment with curved interface is less than 100 nm. Thus, the compressive strain near the edge of such a cut fibre would be, according to Equation 1, less than that in the centre portion of the fibre when the fibre was seated at the knife tip. In other words, bending of this fibre alone would not cause fracture near the fibre edges. As mentioned before, there exists induced shear stress along the fibre–matrix interface which can cause fibres to fracture. The observed fine cracks in Fig. 5a are believed to be due to this mechanism. One can thus use the fine crack dimensions to calculate the maximum shear stress at the fibre–matrix interface by Equation 7.

The average crack spacing and the partial chord length of these fine cracks were measured to be

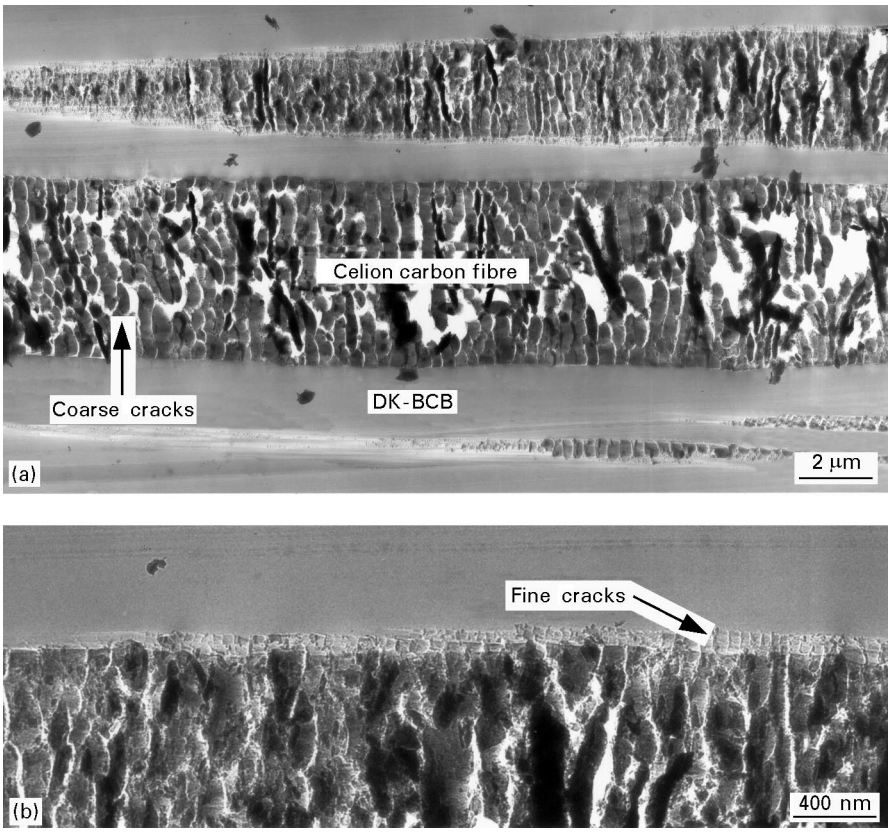


*Figure 5* (a) A transmission electron micrograph of the microstructure of the Celion carbon fibre–(DK-BCB) composite upon ultramicrotomy. (b) An enlargement of the fine cracks at the fibre edge in (a), where the interface is inclined to the surface.

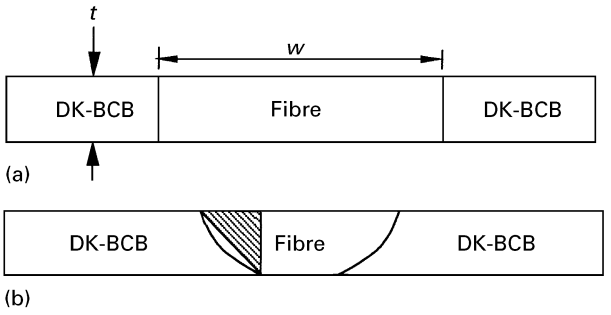


*Figure 6* A schematic diagram of the TEM thin section containing a fibre with interfaces (a) perpendicular and (b) inclined to the section surface. The shaded triangle on the left of (b) is used to calculate the correction factor for the maximum shear stress.

$158 \pm 42$ nm and $180 \pm 57$ nm, respectively. By substituting these values and the compressive strength of 491 MPa obtained above, the calculated maximum shear stress at the carbon fibre–matrix interface is 439 MPa.

Since the fibre geometry is different from that used to derive Equation 7 for the maximum shear stress, corrections for the fibre cross-section and interface areas are needed. Consider one side of the fibre edge as shown in Fig. 6b where a triangle (the shaded area) is used to approximate the real curves interface. Equation 6 suggests that the correction factor is the ratio of cross-section of the fibre to the interface area. For one fine segment which has a triangular cross-section, i.e., $w = 180$ nm, $\lambda = 158$ nm and $t = 100$ nm, the calculated correction factor is 0.28. In other words, the corrected maximum shear stress is 123 MPa, which is higher than the value of 85 MPa [13] obtained by the microbond technique where only a single fibre was used.

It is known that, when the fibres are close together, the strain fields from neighbouring fibres in a composite can interfere with each other, resulting in an increase in the shear stress at the fibre–matrix interface. Also materials under constraint usually exhibit higher strengths than materials without constraint [14]. This may explain why the ultimate shear stress obtained here is higher than that obtained by the microbond technique [13].

On the bases of the argument, a model specimen geometry is schematically shown in Fig. 7a. Upon ultramicrotomy, the fragmentation of the fibre due to bending and induced shear stress at the fibre–matrix interface will create a fracture pattern such as Fig. 7b. Apparently there are other factors of concern when using this microscopy technique. Although the section thickness was set at 100 nm during the ultramicrotomy, which resulted in a thin section having a golden colour under the optical microscope, 15% off the expected thickness is quite common in practice. This would introduce an error of the same order in the calculated compressive strength and interface shear stress. The best strategy to overcome this difficulty is to combine with other techniques for thickness measurement readily available by analytical TEM, such as contamination spots, electron energy loss spectroscopy and convergent beam electron diffraction (only for crystalline materials), to obtain the

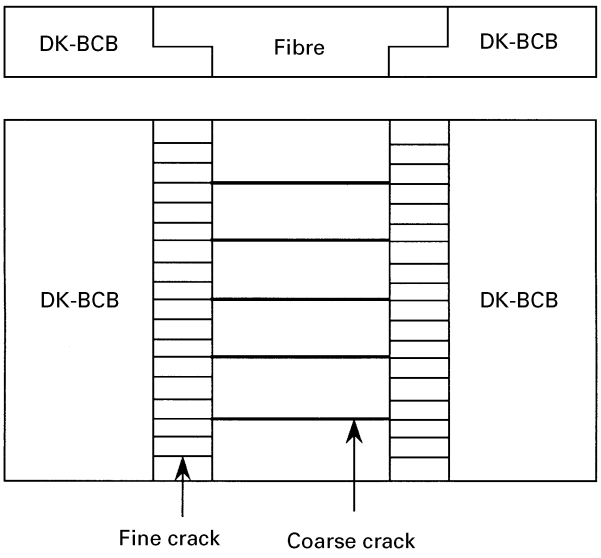


*Figure 7* (a) An idealized specimen geometry for predicting the fracture behaviour of a fibre–reinforced composite. (b) Upon ultramicrotomy, two types of crack, coarse and fine, are produced, corresponding to the failure of the fibre due to bending and induced shear stress at the fibre–matrix interfaces, respectively.

thickness accurately, if necessary. Also in this study we have assumed that the knife tip is perfectly sharp. In reality there are defects present is a diamond knife, especially after it has been used several times. Since a defective knife edge could induce extra stresses in the fibre, this might make accurate analysis more difficult.

## 4. Conclusions

A quantitative method of measuring the compressive strength of a fibre and the ultimate shear stress of the fibre–matrix interface is being developed. This technique uses ultramicrotomy for sample preparation and TEM for image observation. The application of this technique is demonstrated in a Celion carbon–(DK-BCB) composite. The compressive strength of the Celion carbon fibre and the ultimate shear stress of the fibre–matrix interface were measured to be 491 MPa and 123 MPa, respectively. This technique should provide a useful tool to explore the mechanical properties of a composite material on the submicrometre scale, in addition to the other microstructural and compositional information accessible by TEM.

## Acknowledgements

One of the authors (F.S.S.) would like to thank the National Science Council, Taiwan, for financial support of this research under contract NSC 83-0405-E005-001. Thanks are also due to L. Bryton of Dow Chemical Co. for providing the PFCB/Al/Si multilayer sample used in this study.

## References

1. J. L. WALTER, A. H. KING and K. TANGRI (eds), "Structure and Property Relationships for Interfaces" (American Society for Metals, Metals Park, OH, 1991).
2. C. G. PANTANO and E. J. H. CHEN (eds), "Tailored Interfaces in Composite Materials" (Materials Research Society, Pittsburgh, PA, 1989).
3. R. RAJ and S. L. SASS (eds), *J. Physiqe*, **49** (1988).
4. J. A. PASK and A. G. EVANS (eds), "Surfaces and Interfaces in Ceramic and Ceramic–Metal Systems" (Plenum, New York, 1981).
5. C. T. LI, C. L. WHITE and J. A. HORTON, *Acta Metall.* **33** (1984) 213.
6. F.-S. SHIEU, R. RAJ and S. L. SASS, *Acta Metall. Mater.* **38** (1990) 2215.
7. H. L. COX, *Brit. J. Appl. Phys.*, **3** (1952) 72.
8. N. F. DOW, General Electric Co. Report R 63SD61 (1963).
9. A. KELLY, "Strong Solids" (Clarendon, Oxford, 1996).
10. D. C. AGRAWAL and R. RAJ, *Acta Metall.*, **37** (1989) 1265.
11. W. R. TYSON and G. J. DAVIES, *Brit. J. Appl. Phys.* **16** (1965) 199.
12. D. W. RICHERSON, "Modern Ceramic Engineering" (Marcel Dekker, New York, 1982).
13. J. JAKUBOWSKI, Dow Chemical Co., private communications (1993).
14. M. F. ASHBY, F. J. BLUNT and M. BANNISTER, *Acta Metall.* **37** (1989) 1847.

*Received 11 July 1996*
*and accepted 17 June 1997*